DFT Study of the Tetranuclear Lutetium and Yttrium Polyhydride Cluster Complexes $[(C_5Me_4SiMe_3)_4Ln_4H_8]$ (Ln = Lu, Y) that Contain a Four-Coordinate Hydrogen Atom

Yi Luo, Jens Baldamus, Olivier Tardif, and Zhaomin Hou*

Organometallic Chemistry Laboratory, RIKEN (The Institute of Physical and Chemical Research), Hirosawa 2-1, Wako, Saitama 351-0198, Japan, and PRESTO, Japan Science and Technology Agency (JST)

Received March 30, 2005

DFT calculations revealed some unprecedented aspects of the structure of the tetranuclear lutetium and yttrium polyhydride complexes $[(C_5Me_4SiMe_3)_4Ln_4H_8]$ (Ln = Lu, Y). In contrast with the previously described X-ray analysis of $(C_5Me_4SiMe_3)_4Lu_4H_8$, which suffered from a serious disorder problem and showed a C_{2v}-symmetrical structure with one body-centered μ_4-H, two face-capped μ_3-H, and five edge-bridged μ_2-H atoms, the present DFT studies indicated that the optimized Ln_4H_8 core prefers a pseudo-C_{3v}-symmetrical structure with one body-centered μ_4-H, one face-capped μ_3-H, and six edge-bridged μ_2-H atoms. Metal−metal orbital interactions via the hydride bridges were also observed in these complexes. The μ_4-H bonding fashion, a new bonding mode for hydrogen, was well proved by the Wiberg bond indexes and linear overlap bond orders. The X-ray structure of $(C_5Me_4SiMe_3)_4Y_4H_8$, which was solved without suffering from the disorder problems, showed excellent agreement with the theoretical calculations.

Introduction

Metal hydrides are among the most fundamental components in modern inorganic and organic chemistries, with respect to both reactivity and structural variety.[1] So far, tremendous experimental[1a−i] and theoretical[1j,k] studies have been carried out on various metal hydride compounds. For the metal−hydride bonding fashions, the bonding modes of μ_1-H, μ_2-H, μ_3-H, μ_5-H, and μ_6-H have all been well defined by various techniques including neutron diffractions[1e,2] and theoretical calculations. In striking contrast, however, a μ_4-H bonding fashion remained unknown until very recently. During our recent studies on lanthanide polyhydrides,[3] we obtained a tetranuclear lutetium polyhydride complex, $(C_5Me_4SiMe_3)_4Lu_4H_8$ (**1**), which adopts a tetrahedral structure and contains a μ_4-H atom, as shown by X-ray analysis.[3b] This complex could be the first example of a metal hydride compound that possesses four-coordinate hydrogen. However, the X-ray crystal structure of **1** was disordered because of the existence of two crystallographic mirror planes. In view of the general uncertainty in determining the position of a metal hydride atom by X-ray diffraction and of the difficulty to obtain a large crystal for neutron diffraction study, we have now carried out theoretical calculations to further elucidate the metal−hydride connections in **1** and confirm the unprecedented μ_4-H bonding mode. Although the use of computational methods in locating a hydrogen position for transition metal hydride complexes is well known,[1j] its application to lanthanide hydrides, in particular, to polynuclear polyhydrido lanthanide cluster complexes, remained scarce,[4] because of huge computational consumption and complexities in theoretical treatment of the f-elements. In this paper, we report DFT studies on $(C_5Me_4SiMe_3)_4Lu_4H_8$ (**1**) and its yttrium analogue $(C_5Me_4SiMe_3)_4Y_4H_8$ (**2**). The theoretical calculations have not only confirmed the existence of the μ_4-H atom but have also revealed some unprecedented or more detailed structural details such

* To whom correspondence should be addressed. Fax: (81) 48-462-4665. E-mail: houz@riken.jp.

(1) Selected reviews: (a) McGrady, G. S.; Guilera, G. *Chem. Soc. Rev.* **2003**, *32*, 383−392. (b) Suzuki, H. *Eur. J. Inorg. Chem.* **2002**, 1009−1023. (c) Hoskin, A. J.; Stephan, D. W. *Coord. Chem. Rev.* **2002**, *233*−234, 107. (d) Sabo-Etienne, S.; Chaudret, B. *Chem. Rev.* **1998**, *98*, 2077−2092. (e) Bau, R.; Drabnis, M. H. *Inorg. Chim. Acta* **1997**, *259*, 27−50. (f) Ephritikhine, M.; *Chem. Rev.* **1997**, *97*, 2193−2242. (g) Crabtree, R. H. In *Comprehensive Coordination Chemistry*; Wilkinson, G., Gillar, J. A., McCleverty, J. A., Eds.; Pergamon: Oxford, 1987; Vol. 2, p 689. (h) Hlatky, G. G. Crabtree, R. H. *Coord. Chem. Rev.* **1985**, *65*, 1−48. (i) Venanzi, L. M. *Coord. Chem. Rev.* **1982**, *43*, 251−274. (j) Maseras, F.; Lledüs, A.; Clot, E.; Eisenstein, O. *Chem. Rev.* **2000**, *100*, 601−636. (k) Lin, Z.; Hall, M. B. *Coord. Chem. Rev.* **1994**, *135/136*, 845−879.

(2) (a) Bau, R.; Drabnis, M. H. Garlaschelli, L.; Klooster, W. T.; Xie, Z.; Koetzle, T. F.; Martinengo, S. *Science* **1997**, *275*, 1099−1102. (b) Hart, D. W.; Teller, R. G.; Wei, C. W.; Bau, R.; Longoni, G.; Campanella, S.; Chini, P.; Koetzle, T. F. *Angew. Chem., Int. Ed. Engl.* **1979**, *18*, 80−81.

(3) (a) Hou, Z.; Zhang, Y.; Tardif, O.; Wakatsuki, Y. *J. Am. Chem. Soc.* **2001**, *123*, 9216−9217. (b) Tardif, O.; Nishiura, M.; Hou, Z. *Organometallics* **2003**, *22*, 1171−1173. (c) Cui, D.; Tardif, O.; Hou, Z. *J. Am. Chem. Soc.* **2004**, *126*, 1312−1313. (d) Tardif, O.; Hashizume, D.; Hou, Z. *J. Am. Chem. Soc.* **2004**, *126*, 8080−8081. (e) Cui, D.; Nishiura, M.; Hou, Z. *Angew. Chem., Int. Ed.* **2005**, *44*, 959−962.

(4) An ab initio calculation study on a trinuclear lutetium trihydride $Cp_6Lu_3H_3$ complex and its hydride anion $[Cp_6Lu_3H_4]^-$ was recently reported. The calculations were performed by use of effective group potential methodology instead of the real cyclopentadienyl ligand. See: Alary, F.; Heully, J. L.; Poteau, R.; Maron, L.; Trinquier, G.; Daudey, J. P. *J. Am. Chem. Soc.* **2003**, *125*, 11051−11061.

10.1021/om0502382 CCC: $30.25
Publication on Web 08/04/2005

as renewed metal−hydride connectivity and metal−metal interactions, which were unavailable with X-ray analysis.

Computational Details

The 6-31G* basis set was considered for the H and C atoms of the auxiliary π-ligand. To obtain a more accurate core structure, however, 6-311++G(2p) containing two sets of p polarization functions was used for the eight hydrogen atoms involved in the core part. The Stuttgart/Dresden effective "large core" potentials as well as the optimized (4s4p)/[2s2p], (8s7p6d)/[6s5p3d], and (7s6p5d)/[5s4p3d] valence basis sets[5] were used for Si, Y, and Lu, respectively, since it has been theoretically confirmed that 4f-electrons do not explicitly participate in chemical bonding in lanthanide complexes (from La to Lu).[6a] One f polarization function was augmented for the metal atom (exponent of 0.95 for Lu and exponent of 0.84 for Y). The basis set of the Si atom was also augmented by one d polarization function (exponent of 0.28). We call this basis set "BS". Because of huge computational time and memory demand, it is very hard to optimize this heavy system **1** using a "small core" pseudopotential and associated basis in the DFT framework. However, the "larger core" pseudopotential method has been widely applied in the theoretical calculations of lanthanide metal (including Lu) complexes and produced satisfactory geometries for lanthanide (including Lu) complexes.[6b−g,j−l] Due to the large molecular size, each methyl of the realistic ligand η^5-$C_5Me_4SiMe_3$ (Cp′) was replaced by H, which was well accepted in the theoretical calculations of the lanthanide pentamethylcyclopentadienyl complexes.[6b−i] The model complexes $(C_5H_4SiH_3)_4Ln_4H_8$ (Ln = Lu and Y) were optimized at the B3LYP[7]/BS level of theory without symmetry constriction. The geometry optimizations and natural bond orbital (NBO) analysis[8] as well as frequency calculation were performed with the Gaussian 03 program,[9] in which the standard basis sets use linear combinations of Gaussian functions to form the orbitals. The single-point calculations of the optimized geometries were carried out for molecular orbital analysis, using the Amsterdam density functional (ADF) package, which employs Slater-type exponential basis functions centered on the atoms.[10,11] In these single-point calculations, the inner shells on C (1s), Si (including 2p), Y (including 4p), and Lu (including 5p) were treated within the frozen core approximation. Triple-ζ basis sets augmented with two sets of polarization functions were used for the valence shells. The Perdew−Wang exchange and correlation gradient correction (PW91XC) functional[12] planted in the ADF program was used for the single-point calculations.

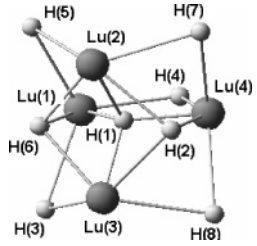

Figure 1. X-ray structure of the Lu_4H_8 core in $(\eta^5$-$C_5Me_4SiMe_3)_4Lu_4H_8$ (**1**), which contains one μ_4-hydrogen (H1), two μ_3-hydrogen (H2, H6), and five μ_2-hydrogen atoms (H3, H4, H5, H7, and H8) (see ref 3b; atoms are renumbered here for comparison with the DFT structure in Figure 2).

Results and Discussion

The X-ray structure of the Lu_4H_8 core in $(C_5Me_4SiMe_3)_4Lu_4H_8$ (**1**) is shown in Figure 1, which possesses one body-centered μ_4-H, two face-capped μ_3-H, and five edge-bridged μ_2-H atoms, as described previously.[3b] Starting from the X-ray crystallographic geometry data of **1**, the full geometry optimization of the model complex $(C_5H_4SiH_3)_4Lu_4H_8$ was performed. To confirm the reliability of the selected theoretical method, the frequency calculation (without anharmonic correction, due to larger molecular size) on the full optimized model complex $(C_5H_4SiH_3)_4Lu_4H_8$ was also performed. The calculated Lu−H bond vibration frequencies, viz., 1267, 1268, 1321, 1333, and 1339 cm^{-1}, are in good agreement with the experimental observations (1261 and 1304 cm^{-1}).[3b] It was also found that the optimized complex molecule $(C_5H_4SiH_3)_4Lu_4H_8$ is really a minimum on the potential energy surface ($N_{imaginary} = 0$, see Supporting Information for the calculated frequencies).

The Lu_4H_8 core structure of the optimized model complex is depicted in Figure 2a. Selected metal−metal distances and angles derived from both DFT and X-ray analyses are summarized in Table 1. The optimized metal−hydrogen contacts in the Lu_4H_8 core are shown in Table 2. The DFT calculation reproduced well the overall tetrahedron skeleton of the Lu_4H_8 core with a

(5) Dolg, M.; Stoll, H.; Savin, A.; Preuss, H. *Theor. Chim. Acta* **1989**, *75*, 173−194. (b) Dolg, M.; Stoll, H.; Preuss, H. *Theor. Chim. Acta* **1993**, *85*, 441−450. (c) Andrae, D.; Haeussermann, U.; Dolg, M.; Stoll, H.; Preuss, H. *Theor. Chim. Acta* **1990**, *77*, 123−141. (d) Bergner, A.; Dolg, M.; Kuechle, W.; Stoll, H.; Preuss, H. *Mol. Phys.* **1993**, *80*, 1431−1441.

(6) (a) Maron, L.; Eisenstein, O. *J. Phys. Chem. A* **2000**, *104*, 7140−7143. (b) Maron, L.; Perrin, L.; Eisenstein, O.; Andersen, R. A. *J. Am. Chem. Soc.* **2002**, *124*, 5614−5615. (c) Maron, L.; Eisenstein, O.; Alary, F.; Poteau, R. *J. Phys. Chem. A* **2002**, *106*, 1797−1801. (d) Maron, L.; Eisenstein, O. *J. Am. Chem. Soc.* **2001**, *123*, 1036−1039. (e) Maron, L.; Perrin, L.; Eisenstein, O. *J. Chem. Soc., Dalton Trans.* **2003**, 4313−4318. (f) Maron, L.; Perrin, L.; Eisenstein, O. *J. Chem. Soc., Dalton Trans.* **2002**, 534−539. (g) Perrin, L.; Maron, L.; Eisenstein, O. *Inorg. Chem.* **2002**, *41*, 4355−4362. (h) Luo, Y.; Selvam, P.; Ito, Y.; Endou, A.; Kubo, M.; Miyamoto, A. *J. Organomet. Chem.* **2003**, *679*, 84−92. (i) Luo, Y.; Selvam, P.; Endou, A.; Kubo, M.; Miyamoto, A. *J. Am. Chem. Soc.* **2003**, *125*, 16210−16212. (j) Kaita, S.; Koga, N.; Hou, Z.; Doi, Y.; Wakatsuki, Y. *Organometallics* **2003**, *22*, 3077−3082. (k) Koga, N. *Theor. Chem. Acc.* **1999**, *102*, 285−292. (l) Zhao, C.; Wang, S.; Phillips, D. L. *J. Am. Chem. Soc.* **2003**, *125*, 15200−15209.

(7) (a) Beck, A. D. *J. Chem. Phys*. **1993**, *98*, 5648−5652. (b) Lee, C. T.; Yang, W. T.; Parr, R. G. *Phys. Rev. B* **1988**, *37*, 785−789.

(8) (a) Foster, J. P.; Weinhold, F. *J. Am. Chem. Soc.* **1980**, *102*, 7211−7218. (b) Reed, A. E.; Weinhold, F. *J. Chem. Phys.* **1983**, *78*, 4066−4073. (c) Reed, A. E.; Weinstock, R. B.; Weinhold, F. *J. Chem. Phys*. **1985**, *83*, 735−746. (d) Reed, A. E.; Curtiss, L. A.; Weinhold, F. *Chem. Rev.* **1988**, *88*, 899−926.

(9) Frisch, M. J.; Trucks, G. W.; Schlegel, H. B.; Scuseria, G. E.; Robb, M. A.; Cheeseman, J. R.; Montgomery, J. A., Jr.; Vreven, T.; Kudin, K. N.; Burant, J. C.; Millam, J. M.; Iyengar, S. S.; Tomasi, J.; Barone, V.; Mennucci, B.; Cossi, M.; Scalmani, G.; Rega, N.; Petersson, G. A.; Nakatsuji, H.; Hada, M.; Ehara, M.; Toyota, K.; Fukuda, R.; Hasegawa, J.; Ishida, M.; Nakajima, T.; Honda, Y.; Kitao, O.; Nakai, H.; Klene, M.; Li, X.; Knox, J. E.; Hratchian, H. P.; Cross, J. B.; Bakken, V.; Adamo, C.; Jaramillo, J.; Gomperts, R.; Stratmann, R. E.; Yazyev, O.; Austin, A. J.; Cammi, R.; Pomelli, C.; Ochterski, J. W.; Ayala, P. Y.; Morokuma, K.; Voth, G. A.; Salvador, P.; Dannenberg, J. J.; Zakrzewski, V. G.; Dapprich, S.; Daniels, A. D.; Strain, M. C.; Farkas, O.; Malick, D. K.; Rabuck, A. D.; Raghavachari, K.; Foresman, J. B.; Ortiz, J. V.; Cui, Q.; Baboul, A. G.; Clifford, S.; Cioslowski, J.; Stefanov, B. B.; Liu, G.; Liashenko, A.; Piskorz, P.; Komaromi, I.; Martin, R. L.; Fox, D. J.; Keith, T.; Al-Laham, M. A.; Peng, C. Y.; Nanayakkara, A.; Challacombe, M.; Gill, P. M. W.; Johnson, B.; Chen, W.; Wong, M. W.; Gonzalez, C.; Pople, J. A. *Gaussian 03*, Revision C.01; Gaussian, Inc.: Wallingford, CT, 2004.

(10) *ADF2004.01, SCM*; Theoretical Chemistry, Vrije Universiteit, Amsterdam: The Netherlands, http://www.scm.com.

(11) (a) te Velde, G.; Bickelhaupt, F. M.; van Gisbergen, S. J. A.; Fonseca Guerra, C.; Baerends, E. J.; Snijders, J. G.; Ziegler, T. *J. Comput. Chem.* **2001**, *22*, 931−967. (b) Fonseca Guerra, C.; Snijders, J. G.; te Velde, G.; Baerends, E. J. *Theor. Chem. Acc.* **1998**, *99*, 391−403.

(12) (a) Perdew, J. P.; Wang Y. *Phys. Rev. B* **1986**. *33*, 8800−8802. (b) Perdew, J. P.; Chevary, J. A.; Vosko, S. H.; Jackson, K. A.; Pederson, M. R.; Singh, D. J.; Fiolhais, C. *Phys. Rev. B* **1992**. *46*, 6671−6687.

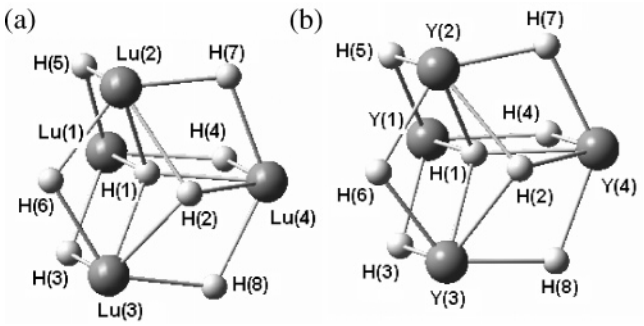

Figure 2. (a) DFT-optimized structure of the Lu_4H_8 core in $(\eta^5\text{-}C_5H_4SiH_3)_4Lu_4H_8$ (a model for **1**); (b) DFT-optimized structure of the Y_4H_8 core in $(\eta^5\text{-}C_5H_4SiH_3)_4Y_4H_8$ (a model for **2**). There are one μ_4-hydrogen (H1), one μ_3-hydrogens (H2), and six μ_2-hydrogen atoms (H3−H8) in each structure.

Table 1. Selected Metal−Metal Distances (Å) and Angles (deg) for the Lu_4H_8 Cores in the DFT-Optimized Complex $(\eta^5\text{-}C_5H_4SiH_3)_4Lu_4H_8$ and the X-ray Crystal Structure of 1[a]

	DFT	X-ray[b]	deviation
Lu(1)···Lu(2)	3.570	3.368	0.202
Lu(1)···Lu(3)	3.570	3.368	0.202
Lu(1)···Lu(4)	3.573	3.464	0.109
Lu(2)···Lu(3)	3.398	3.276	0.122
Lu(2)···Lu(4)	3.392	3.368	0.024
Lu(3)···Lu(4)	3.395	3.368	0.027
Lu(2)−Lu(1)−Lu(3)	56.84	58.19	1.35
Lu(2)−Lu(1)−Lu(4)	56.78	59.06	2.28
Lu(3)−Lu(1)−Lu(4)	56.79	59.06	2.27
Lu(1)−Lu(2)−Lu(4)	61.65	61.89	0.24
Lu(1)−Lu(2)−Lu(3)	61.61	60.90	0.71
Lu(3)−Lu(2)−Lu(4)	59.99	60.90	0.91
Lu(1)−Lu(3)−Lu(2)	61.56	60.90	0.66
Lu(1)−Lu(3)−Lu(4)	61.62	61.89	0.27
Lu(2)−Lu(3)−Lu(4)	59.97	60.90	0.93
Lu(1)−Lu(4)−Lu(2)	61.57	59.06	2.51
Lu(1)−Lu(4)−Lu(3)	61.59	59.06	2.53
Lu(2)−Lu(4)−Lu(3)	60.04	58.19	1.85

[a] Atom labeling defined in Figures 1 and 2a. [b] X-ray data are taken from ref 3b.

Table 2. DFT-Optimized Ln−H Contacts (Å) in $(\eta^5\text{-}C_5H_4SiH_3)_4Ln_4H_8$[a]

bond	Ln = Lu	Ln = Y
Ln(1)−H(1)	2.083	2.127
Ln(2)−H(1)	2.162	2.210
Ln(3)−H(1)	2.161	2.212
Ln(4)−H(1)	2.158	2.210
Ln(2)−H(2)	2.289	2.332
Ln(3)−H(2)	2.296	2.322
Ln(4)−H(2)	2.298	2.324
Ln(1)−H(3)	2.122	2.151
Ln(3)−H(3)	2.164	2.191
Ln(1)−H(4)	2.121	2.151
Ln(4)−H(4)	2.163	2.192
Ln(1)−H(5)	2.121	2.150
Ln(2)−H(5)	2.163	2.191
Ln(1)···H(6)	3.678	3.764
Ln(2)−H(6)	2.105	2.132
Ln(3)−H(6)	2.103	2.130
Ln(2)−H(7)	2.103	2.129
Ln(4)−H(7)	2.103	2.129
Ln(3)−H(8)	2.102	2.131
Ln(4)−H(8)	2.100	2.130

[a] Atom labeling defined in Figure 2.

body-centered μ_4-H atom. However, a careful examination revealed some significant differences between the theoretical and the X-ray structures. In sharp contrast with the X-ray structure, which showed two face-capped μ_3-H atoms H(2) and H(6) (Figure 1), the DFT-optimized structure contains only one face-capped μ_3-H atom, H(2), whereas the Lu(1)−H(6) distance becomes as long as 3.678 Å after optimization, indicating that there is virtually no bonding interaction between Lu(1) and H(6) in the optimized Lu_4H_8 core (Figure 2a and Table 2). The mirror planes observed in the X-ray crystallographic structure (C_{2v} symmetry), which was actually the cause of the disorder problem in the X-ray analysis, do not exist in the optimized structure. Instead, the optimized Lu_4H_8 core adopts a pseudo-C_{3v} symmetry, in which there is a quasi 3-fold axis passing through Lu(1), the body-centered μ_4-H(1), and the face-capped μ_3-H(2) ($\angle$Lu(1)−H(1)−H(2) = 179.8°) (Figure 2a).

Table 3. Natural Charge Population and the Electron Configuration of Atomic Orbitals in the Ln_4H_8 Core of $(\eta^5\text{-}C_5H_4SiH_3)_4Ln_4H_8$[a]

	Ln = Lu		Ln = Y	
atom[b]	charge	configuration	charge	configuration
Ln(1)	1.75	$6s^{0.27}5d^{0.96}\,6d^{0.04}$	1.72	$4d^{1.01}6s^{0.24}5d^{0.01}6d^{0.03}$
Ln(2)	1.56	$6s^{0.26}5d^{1.17}\,6d^{0.03}$	1.55	$4d^{1.20}6s^{0.24}5d^{0.01}6d^{0.03}$
Ln(3)	1.56	$6s^{0.26}5d^{1.17}\,6d^{0.04}$	1.55	$4d^{1.20}6s^{0.24}5d^{0.01}6d^{0.03}$
Ln(4)	1.56	$6s^{0.26}5d^{1.17}\,6d^{0.04}$	1.55	$4d^{1.20}6s^{0.24}5d^{0.01}6d^{0.03}$
H(1)	−0.46	$1s^{1.46}$	−0.49	$1s^{1.49}$
H(2)	−0.42	$1s^{1.42}$	−0.43	$1s^{1.43}$
H(3)	−0.51	$1s^{1.51}$	−0.52	$1s^{1.52}$
H(4)	−0.50	$1s^{1.50}$	−0.51	$1s^{1.51}$
H(5)	−0.50	$1s^{1.51}$	−0.52	$1s^{1.52}$
H(6)	−0.48	$1s^{1.48}$	−0.48	$1s^{1.48}$
H(7)	−0.48	$1s^{1.48}$	−0.49	$1s^{1.49}$
H(8)	−0.48	$1s^{1.48}$	−0.48	$1s^{1.48}$

[a] The calculations were based on the optimized geometries. [b] Atom labeling is defined in Figure 2.

Consistent with the absence of the Lu(1)−H(6) bond in the optimized structure, the calculated values for the Lu(1)···Lu(i) (i = 2, 3, 4) and Lu(2)···Lu(3) metal−metal distances are significantly longer (>0.1 Å) than those found by X-ray analysis, while the Lu(2)···Lu(4) and Lu(3)···Lu(4) separations are in good agreement between theoretical and X-ray analyses (with deviation ≤0.027 Å) (see Figures 1 and 2a and Table 1). As a result or compensation of breaking of the Lu(1)−H(6) bond, H(6) is now coplanar with Lu(2), H(7), Lu(4), H(8), and Lu(3) (Figure 2),[13] which thus leads to better orbital overlaps (vide infra). The μ_4-H hydrogen H(1) is not equally bonded to the four metal atoms, with the Lu(1)−H(1) bond length (2.083 Å) being slightly shorter than those of the Lu(2)−H(1), Lu(3)−H(1), and Lu(4)−H(1) bonds (2.158−2.162 Å) (Table 2). Similarly, H(3), H(4), and H(5) are also closer to Lu(1) than to Lu(3), Lu(4), and Lu(2), respectively. The lack of symmetry in these Lu−H bonds could be ascribed to the fact that the coordination number of Lu(1) (bonding to four H atoms) is one less than that of other Lu atoms (each being bonded to five H atoms) in the optimized Lu_4H_8 core. The difference in the coordination number of four Lu atoms indicated their different bonding situations, which are also reflected by the natural charge and valence electron population (Table 3) obtained from NBO analysis.[8] As shown in Table 3, Lu(1) carries more positive charge (1.75) compared to the other three Lu atoms (1.56), which indicates the stronger bonding of

(13) The maximum deviation from the least-squares plane formed by the six atoms H(6), Lu(2), H(7), Lu(4), H(8), and Lu(3) is 0.02 Å.

Table 4. Wiberg Bond Indexes (WBI) and Linear Overlap Bond Orders (LOBO) for the Ln_4H_8 Core in DFT-Optimized $(\eta^5\text{-}C_5H_4SiH_3)_4Ln_4H_8$[a]

	Ln = Lu	Ln = Y
bond	WBI (LOBO)	WBI (LOBO)
Ln(1)···Ln(2)	0.10 (0.27)	0.10 (0.18)
Ln(1)···Ln(4)	0.10 (0.27)	0.11 (0.19)
Ln(1)···Ln(3)	0.10 (0.27)	0.10 (0.19)
Ln(2)···Ln(4)	0.13 (0.34)	0.14 (0.27)
Ln(2)···Ln(3)	0.13 (0.34)	0.14 (0.27)
Ln(3)···Ln(4)	0.13 (0.34)	0.15 (0.28)
H(1)−Ln(1)	0.19 (0.24)	0.20 (0.25)
H(1)−Ln(2)	0.19 (0.25)	0.20 (0.25)
H(1)−Ln(3)	0.19 (0.25)	0.20 (0.26)
H(1)−Ln(4)	0.19 (0.25)	0.20 (0.26)
H(2)−Ln(2)	0.26 (0.30)	0.26 (0.31)
H(2)−Ln(3)	0.25 (0.31)	0.26 (0.31)
H(2)−Ln(4)	0.27 (0.31)	0.27 (0.32)
H(6)−Ln(1)	0.01 (0.03)	0.02 (0.03)
H(6)−Ln(2)	0.34 (0.35)	0.36 (0.39)
H(6)−Ln(3)	0.35 (0.36)	0.35 (0.38)
H(i)−Ln (average) (i = 3, 4, 5, 7, and 8)	0.34 (0.36)	0.36 (0.37)

[a] The atom labeling is defined in Figure 2.

Table 5. Atomic Orbital Contribution (%) to HOMO−8 and HOMO−11[a]

	$(\eta^5\text{-}C_5H_4SiH_3)_4Lu_4H_8$			$(\eta^5\text{-}C_5H_4SiH_3)_4Y_4H_8$	
orbital	HOMO−8	HOMO−11	orbital	HOMO−8	HOMO−11
μ_2-H(1s)	30.1	47.2	μ_2-H(1s)	32.4	50.7
μ_3-H(1s)	23.1	/	μ_3-H(1s)	23.7	/
μ_4-H(1s)	10.9	19.4	μ_4-H(1s)	10.6	14.6
Lu(5d)	33.2	23.8	Y(4d)	30.3	21.4
Lu(6s)	2.7	9.6	Y(5s)	3.0	13.3

[a] For each metal valence shell, the contribution contains that from all four metal atoms.

Lu(1) with its ligands. The 5d valence shell of Lu(1) possesses less electron population than that of Lu(i) (i = 2, 3, or 4). The latter as an electron acceptor has more than one electron.

It is also noteworthy that the bond lengths between the four-coordinate hydrogen atom H(1) and the four Lu atoms (Lu−H(1) = 2.083−2.162 Å) are significantly shorter than those between the three-coordinate hydrogen atom H(2) and Lu(2), Lu(3), or Lu(4) (Lu−H(2) = 2.289−2.298 Å), probably owing to the restriction of the tetrahedron cavity. The μ_2-H−Lu bond distances in the H(6)−Lu(2)−H(7)−Lu(4)−H(8)−Lu(3) six-membered ring plane are almost the same (2.100−2.105 Å) and are significantly shorter than other μ_2-H−Lu bond distances (Lu−H(i) = 2.121−2.164 Å, i = 3, 4, 5) in the Lu_4H_8 core (Figure 2a and Table 2). The difference in Lu−H contacts indicated different bonding behavior of the hydrogen atoms, which is also reflected by the charge population on various hydrogen atoms (Table 3).

The Wiberg bond indexes (WBI) and linear overlap bond orders (LOBO) are summarized in Table 4. A bond index of 0.19 and overlap bond orders of 0.24−0.25 were found between H(1) and the four Lu atoms (Table 4), which strongly suggests that H(1) is indeed bonded to all four Lu atoms. Similarly, the μ_3-H(2)−Lu and μ_2-H−Lu bonds were also supported by their bond indexes and bond orders (Table 4). In contrast, however, the bond index (0.01) and bond order (0.03) for H(6)−Lu(1) do not imply any bonding interaction between H(6) and Lu(1). These results are in good agreement with those found in the geometry analysis described above. Moreover, a bond index of 0.10 and an overlap bond order of 0.27 were found between Lu(1) and the other three Lu atoms. Similarly, a bond index of 0.13 and an overlap bond order of 0.34 were observed among Lu(2), Lu(3), and Lu(4). These results strongly suggest that there are significant bonding interactions among all four metal atoms.[14]

Table 6. Selected Metal−Metal Distances (Å) and Angles (deg) for the DFT-Optimized Y_4H_8 Core and the X-ray Y_4H_8 Core[a]

	DFT	X-ray	deviation
Y(1)···Y(2)	3.655	3.621	0.034
Y(1)···Y(3)	3.653	3.597	0.056
Y(1)···Y(4)	3.653	3.593	0.060
Y(2)···Y(3)	3.477	3.479	0.002
Y(2)···Y(4)	3.477	3.462	0.015
Y(3)···Y(4)	3.476	3.460	0.016
Y(2)−Y(1)−Y(3)	56.83	57.63	0.80
Y(2)−Y(1)−Y(4)	56.81	57.36	0.55
Y(3)−Y(1)−Y(4)	56.82	57.52	0.70
Y(1)−Y(2)−Y(4)	61.57	60.93	0.64
Y(1)−Y(2)−Y(3)	61.55	60.84	0.71
Y(3)−Y(2)−Y(4)	59.99	59.87	0.12
Y(1)−Y(3)−Y(2)	61.62	61.53	0.09
Y(1)−Y(3)−Y(4)	61.60	61.19	0.41
Y(2)−Y(3)−Y(4)	60.00	59.87	0.13
Y(1)−Y(4)−Y(2)	61.62	61.72	0.10
Y(1)−Y(4)−Y(3)	61.58	61.29	0.29
Y(2)−Y(4)−Y(3)	60.02	60.35	0.33

[a] Atom labeling is defined in Figure 2b.

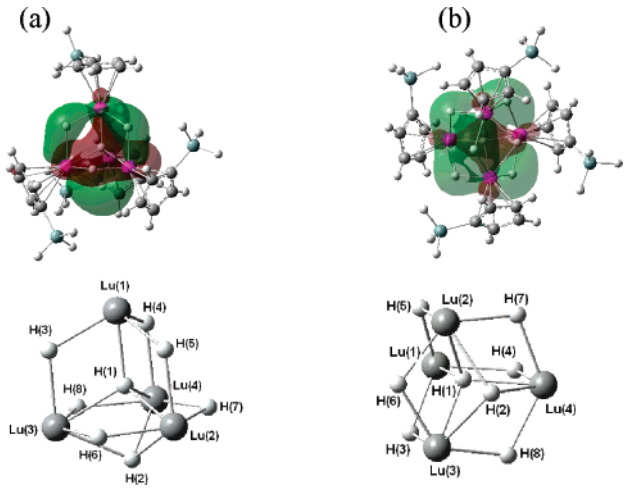

Figure 3. Molecular orbital (MO) isosurfaces (top) of $(\eta^5\text{-}C_5H_4SiH_3)_4Lu_4H_8$ (a model for **1**) and the corresponding views of the Lu_4H_8 core (bottom). (a) HOMO−8. (b) HOMO−11.

For a better understanding of the μ_4-H(1)−Lu bonds and the metal−metal interactions, the HOMO−8 and HOMO−11 molecular orbitals are shown in Figures 3a and 3b, respectively, which clearly demonstrate the bonding between the μ_4-H(1) atom and the four Lu atoms and the interactions among the four Lu atoms through the orbital overlaps between the 1s orbital of the H atom(s) and the s−d hybrid orbitals of the Lu atoms. The atomic orbital contributions shown in Table 5 also illustrate these bondings. Apparently, the μ_4-H,

(14) (a) Choi, S. H.; Lin, Z. *J. Organomet. Chem.* **2000**, *608*, 42−48. (b) Gleiter, R.; Schimanke, H.; Silverio, S. J.; Buechner, M.; Huttner, G. *Organometallics* **1996**, *15*, 5635−5640. (c) Lain, L.; Torre, A.; Bochicchio, R. *J. Phys. Chem. A* **2004**, *108*, 4132−4137. (d) Kovacs, A.; Frenking, G. *Organometallics* **2001**, *20*, 2510−2524.

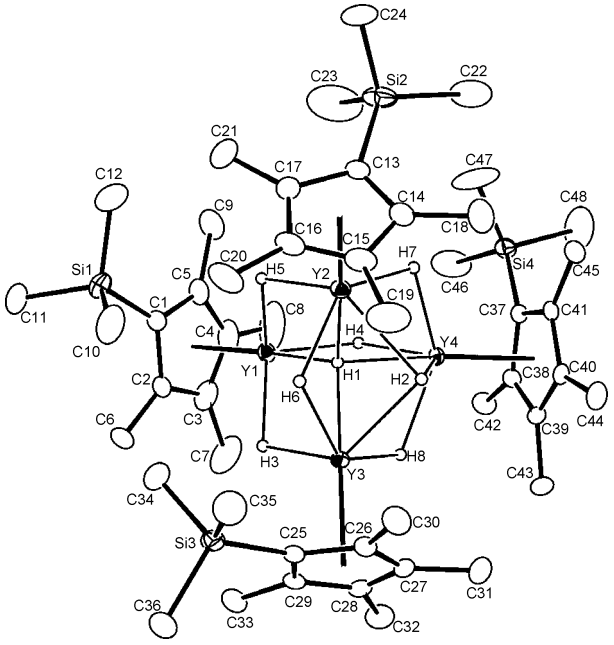

Figure 4. ORTEP view of **2** with ellipsoids shown at the 30% level of probability. Hydrogen atoms in the Cp′ ligands are omitted for clarity.

μ_3-H, and μ_2-H hydride bridges play a very important role in the formation of the metal−metal interactions.

To see if the above-optimized Lu_4H_8 core structure (e.g., pseudo-C_{3v} symmetry, μ_4-H, metal−metal interactions, etc.) is general to tetranuclear metal polyhydrides having a "M_4H_8" core, similar calculations on the analogous yttrium complex $(\eta^5\text{-}C_5H_4SiH_3)_4Y_4H_8$, a model compound of $(\eta^5\text{-}C_5Me_4SiMe_3)_4Y_4H_8$ (**2**),[15] were also performed. It was found that the optimized Y_4H_8 core structure is almost the same as that of Lu_4H_8 (see Figure 2 and Tables 2 and 6). The bonding features similar to those in complex $(\eta^5\text{-}C_5H_4SiH_3)_4Lu_4H_8$ were also supported by the natural charge population (Table 3) and Wiberg bond indexes and line overlap bond orders (Table 4) as well as the atomic orbital contributions (Table 5). Fortunately, the X-ray crystal structure of the yttrium complex $(\eta^5\text{-}C_5Me_4SiMe_3)_4Y_4H_8$ (**2**) has now been successfully solved without suffering from the disorder problem observed in **1** (Figure 4). An excellent agreement between the X-ray structure of **2** and the optimized structure of the model compound $(\eta^5\text{-}C_5H_4SiH_3)_4Y_4H_8$ was observed, with a deviation in Y···Y distances being less than 0.06 Å and a deviation in ∠Y−Y−Y less than 0.9° (Table 6). These findings strongly support our calculation results.

(15) The formation of the tetranuclear yttrium polyhydride complex $(\eta^5\text{-}C_5Me_4SiMe_3)_4Y_4H_8$ (**2**) was briefly mentioned previously. See ref 3c.

Conclusion

The DFT calculations have revealed unprecedented details on the structure of the lanthanide polyhydride cluster complexes $(C_5Me_4SiMe_3)_4Ln_4H_8$ (Ln = Lu and Y). In contrast with the previously described X-ray analysis of $(C_5Me_4SiMe_3)_4Lu_4H_8$ (**1**), which suffered from serious disorder problems and showed a C_{2v}-symmetrical structure with one body-centered μ_4-H, two face-capped μ_3-H, and five edge-bridged μ_2-H atoms, the theoretical calculations have indicated that a pseudo-C_{3v}-symmetrical structure with one body-centered μ_4-H, one face-capped μ_3-H, and six edge-bridged μ_2-H atoms is preferred for the Lu_4H_8 core. Four-coordinate hydrogen (μ_4-H) has been proved for the first time by theoretical calculations. Metal−metal interactions via the hydride bridges have also been found, which, as far as we are aware, represents the first example of observation of metal−metal orbital interactions in a lanthanide complex. This work demonstrates that DFT can be a powerful tool for structure prediction and examination of lanthanide polyhydride complexes.

Acknowledgment. This work was partly supported by a Grant-in-Aid for Scientific Research on Priority Areas (No. 14078224, "Reaction Control of Dynamic Complexes") (to Z.H.) and for Young Scientists (No. 17750061) (to Y.L.) from the Ministry of Education, Culture, Sports, Science and Technology of Japan. We thank RIKEN Advanced Center for Computing and Communication for providing computational resources.

Supporting Information Available: Tables and figures giving the distances between the metal and the Cp′ ligand, molecular orbital isosurfaces of $(C_5H_4SiH_3)_4Y_4H_8$, optimized coordinates, calculated frequencies, and experimental details on the synthesis and X-ray crystallographic study of **2**. This material is available free of charge via the Internet at http://pubs.acs.org.

OM0502382